

*IN-SITU* RAMAN SPECTROSCOPY STUDIES OF METAL-ION COMPLEXATION  
BY 8-HYDROXYQUINOLINE COVALENTLY BOUND TO SILICA SURFACES

Rory H. Uibel and Joel M. Harris\*  
Department of Chemistry  
University of Utah  
315 South 1400 East  
Salt Lake City, UT 84112-0850

ABSTRACT

Raman spectroscopy is applied to an investigation of the interfacial chemistry of silica-immobilized 8-hydroxyquinoline (8HQ) for binding of metal ions over a wide range of solution conditions. Since the derivatized silica has a high specific binding capacity, the mass of silica equilibrated with solution needs to be small for studies of reactions with trace-level ( $\mu\text{M}$ ) metal ions; otherwise, the solution volume required to reach equilibrium becomes excessive. To address this problem, a small-volume flow cell is designed for this work using a fiber-optic Raman probe inserted directly into the packed end of a microcolumn, allowing excitation and collection of Raman scattering from less than 10 mg of derivatized silica. This cell is attached to a flow system that allows control of solution conditions while the response of the 8HQ-silica material is acquired by continuous monitoring of Raman scattering from the sample. Raman spectra of the deprotonated, neutral, protonated, and copper-complexed forms of the ligand can be distinguished allowing proton-transfer and metal-ion binding reactions of the ligand to be investigated. To account for the effects of changing surface potential on these reactions, zeta-potential measurements are made on the 8HQ-silica particles under the same solution conditions that are employed in the Raman scattering measurements. The observed pH dependence of metal-ion binding was corrected for the effect of surface-potential using the Boltzmann Equation, and the resulting equilibrium constant for binding of  $\text{Cu}^{2+}$  was independent of metal-ion concentration over a 100-fold range from  $30\mu\text{M}$  to  $5\text{mM}$ .

Silica gels that are chemically modified with surface-immobilized reagents can be used for the clean-up of metals from waste streams, for separation of different metal-ion species, or preconcentration of metal ions for trace-level detection. Recent progress has been made in synthesis of new ligands that can be bound onto silica supports [1-6]. One of the most widely used silica-immobilized metal chelating reagents used for preconcentration of trace elements is 8-hydroxyquinoline (8HQ) [7-10]. This ligand exhibits a high affinity for a variety of transition metals while rejecting the alkaline-earth species [10]. Over 60 metals can react with 8HQ to form complexes, with formation constants in solution ranging from  $10^4$  ( $\text{Ba}^{2+}$ ) to  $10^{49}$  ( $\text{Ga}^{3+}$ ) [10,11].

Detailed knowledge of the chemistry between the interaction of metal ions with the immobilized 8HQ is critical to its successful application. Our understanding of the chemistry of metal-ion binding of silica-immobilized 8HQ has generally relied on detection of solution-phase analyte breakthrough or elution from the end of a packed column [8,9,12-16]. Jezorek and Freiser [8] used these methods to report the first pH effects for metal-ion complexation with 8HQ immobilized to controlled-pore glass (CPG). Marshall and Mottola [9] derived a simple synthetic route to immobilize 8HQ onto CPG using a diazo-coupling reaction to a surface-bound aromatic amine; they determined the  $\text{pK}_A$  of the surface-bound ligand and binding capacities for various metal ions. Cantwell and coworkers [14-16] accounted for the calcium binding equilibria of immobilized 8HQ using a site-binding model that included the effects of the silica surface potential. A pulsed elution technique was recently developed by Howard and Holcombe [17] where a frontal chromatography model was applied to predict the behavior of immobilized 8HQ in flow systems.

While column elution studies have produced important information about the binding capacity of immobilized 8HQ ligands, less progress has been made in developing *in-situ* spectroscopic methods to detect the various forms of the ligand on the silica surface. Fluores-

cence spectroscopy has been adapted to flow injection methods for *in-situ* detection of aluminum-ion complexation to silica immobilized 8HQ [18]. *In-situ* absorbance measurements conducted through a thin layer of immobilized 8HQ were used to determine the second acid dissociation constant of the ligand [19]. In general, electronic absorption or fluorescence measurements of immobilized 8HQ cannot readily distinguish the various forms of the ligand. Vibrational spectroscopy provides the opportunity to distinguish these forms and to probe their structure. In recent work from our laboratory [20], we demonstrated that *in situ* fiber-optic Raman spectroscopy was capable of distinguishing the protonated, neutral and metal-ion complexed forms of silica-immobilized 8HQ.

The purpose of the present work is to apply *in-situ* Raman spectroscopy in an investigation of the interfacial chemistry of silica-immobilized 8HQ for binding of metal ions over a wide range of solution conditions. Since the derivatized silica has a high specific binding capacity (typically  $\sim 0.2$  mmol/g), the mass of silica to be equilibrated with solution needs to be small for studies of reactions with trace-level ( $\mu\text{M}$ ) metal ions; otherwise, the solution volume required to reach equilibrium becomes excessive. For example, a 0.5 g sample of 8HQ-derivatized silica reacting with a 10  $\mu\text{M}$  solution of a target metal ion would require 10 L of solution to reach equilibrium under strong binding conditions. To address this problem, a flow cell is designed for this work using a fiber-optic Raman probe inserted directly into the packed end of a microcolumn, allowing excitation and collection of Raman scattering from less than 10 mg of derivatized silica. This cell is attached to a flow system that allows control of solution conditions while the response of the 8HQ-silica material is acquired by continuous monitoring of Raman scattering from the sample. To account for the effects of changing surface potential on the proton-transfer and metal-ion binding reactions of the immobilized ligands, zeta-potential measurements are made on the 8HQ-silica particles under the same solution conditions that are employed in the Raman scattering measurements.

## EXPERIMENTAL SECTION

**Synthesis of Surface Immobilized 8HQ** The synthesis of the silica-immobilized 8HQ (see Figure 1) was carried out using the procedure developed by Marshall and Mottola [9] using a diazonium salt of a silica-immobilized aromatic amine to immobilize the 8HQ. The specific reagents and conditions used for this synthesis were described in an earlier publication [20]. The 60  $\mu\text{m}$  particle diameter, 60  $\text{\AA}$  pore diameter silica gel (EM Science) was first derivatized with p-aminophenyltrimethoxysilane; elemental analysis (MHW Laboratories, Phoenix) of the silica-bound aromatic amine yielded 1.54% C and 0.26% N which corresponds to a surface coverage of 0.36  $\mu\text{mol}/\text{m}^2$ , based on the specific surface area (550  $\text{m}^2/\text{g}$ ) of the silica gel. Subsequent reaction of the diazonium salt of the aromatic amine with 8HQ yields a final silica product containing 3.26% C and 0.69% N. Subtracting the mass of carbon and nitrogen of the original aromatic amine anchor groups from the final product values gives the increase in carbon and nitrogen derived from binding 8HQ to the surface; the carbon and nitrogen are both consistent with an 8HQ specific capacity of 0.15 mmol/g or a surface coverage of 0.28  $\mu\text{mol}/\text{m}^2$ . This result indicates that  $\approx 80\%$  of the phenylamine anchor groups bind 8HQ in the final product. The surface coverage of the bound 8HQ is approximately 1/10 of a full monolayer, corresponding to an average distance of  $\sim 24 \text{\AA}$  between ligands.

**Preparation of Buffers** The buffer system for this work needed to have spectroscopic transparency, a known and constant ionic strength, negligible fluorescence, and minimal complexation with copper ions in the pH = 1-8 range. For these reasons, the buffers were prepared from hydrochloric acid (Fisher), chloroacetic acid ( $\text{pK}_A = 2.88$  [21]), acetic acid ( $\text{pK}_A = 4.76$  [21]), ACES (N-(2-acetamido)-2-aminoethanesulfonate,  $\text{pK}_A = 6.99$  [21]), and phosphate,  $\text{pK}_{A2} = 7.21$  [21]), titrated with sodium chloroacetate, sodium acetate, and sodium hydroxide (Aldrich). Sodium chloride was added to yield a constant ionic strength of 0.1M. The  $\text{Cu}^{2+}$  concentrations were sufficiently low so that they did not affect the ionic strength of the buffered

solutions. The pH of each solution was verified at 23 °C with a pH meter.

**Zeta Potential Measurements.** A Phase Analysis Light-Scattering Zeta-Potential Analyzer (Brookhaven Instruments Corp.) was used to determine the zeta ( $\zeta$ ) potential of the silica-immobilized 8HQ at various solution pH values and  $\text{Cu}^{2+}$  concentrations. The  $\zeta$  potential is measured at the interface between the moving particle and the liquid known as the shear plane [22]. This system measures the optical phase shift of the particles migrating under the influence of an electrical field of  $\sim 8\text{V/cm}$ . The 8HQ-derivatized silica gel used for these measurements was a LiChrosorb Si100 (EM Separations) chosen for smaller ( $5\ \mu\text{m}$ ) particle diameter to avoid settling during the light scattering measurements; for equivalent surfaces, the measured  $\zeta$  potential does not depend on particle size [22]. Measurements were carried out at  $\text{Cu}^{2+}$  concentrations ranged from 0 M, 30  $\mu\text{M}$ , 600  $\mu\text{M}$ , and 5 mM, and solution pH was varied from 2.3 to 9.8 to cover the range of proton-transfer and metal-ion binding equilibria. The ionic strength was held constant at 0.1 M so as to not change the Debye length of the double layer. An average of six runs was reported for each measurement.

**Raman Measurements** The Raman instrument (shown in Figure 2A) was previously described [20]; briefly, a 647.1 nm line from a Krypton ion laser (Coherent, Innova 90-K) was passed through a dove prism, a plano convex lens ( $f=1.0\ \text{m}$ ) and a 0.5 mm pinhole to remove plasma lines. The beam was focused onto a bifurcated fiber optic probe (Fiberguide Industries) using a multimode fiber coupler (Newport) and a 10X microscope objective. The bifurcated fiber optic probe consisted of 44 silica collection fibers ( $100\ \mu\text{m}$ ) surrounding a central excitation fiber. The light-collection fibers were arranged in a linear array, collimated by an F/1.3 camera lens (JML Optics), and focused by a plano-convex lens ( $f=175\ \text{mm}$ ) onto the entrance slit of a F/7 single-stage 0.5 m spectrograph (Spex). A holographic notch filter (Kaiser) for the 647.1 nm line was placed between the collection and focusing lenses to remove Rayleigh and specular

scattering. The Raman scattering was detected with a 1024 X 256 TE-cooled CCD (Andor). Samples were typically excited with ~100 mW of incident laser power, and scattering was integrated in six accumulations of 20 seconds each.

The micro flow cell used in the metal-ion binding studies was a modified stainless steel ¼ inch Swagelock Tee shown in Figure 2B. The cell was assembled by inserting the common end of the fiber optic into one side of the Tee, and then inserting a polished 0.075 inch inner diameter tubing into the other side of the Tee. The fibers and small diameter tubing were pressed together, and connectors on the ends of the Tee held these parts in place. The side-arm of the Tee was used as the solution outlet. The small diameter tubing was then filled with ~10 mg of dry surface-modified silica particles and connected to the flow system. An acetate buffer solution (pH = 4.7) was flowed through the column at a rate of 2 mL/min with an HPLC pump (Beckman, Model 110A) to pack the dry silica up against the fiber optic. Changes in the 8HQ Raman signal were used to monitor the packing of the silica, and typically times for the Raman signal to reach steady state were around 10 minutes. The acetate buffer was pumped at 2 mL/min for another 30 minutes to ensure that all of the silica particles had packed as closely as possible. To equilibrate metal-ion containing samples with the silica surface, typically 100 mL of buffered solution were pumped through the column at 1.0 mL/min. To remove metal ions bound to the surface, aqueous 0.1 M HCl was used as an eluent to reset the surface for subsequent experiments.

**Data Analysis.** Prior to data analysis, an observed Raman spectrum was baseline-subtracted by fitting the fluorescence background to a cubic equation using ten points that were varied until the difference spectrum contained a flat baseline with zero offset; the resulting difference spectrum was then normalized. Classical least squares regression analysis was employed to test complexation models and to resolve the spectra of the different ligand components. Raman spectra were collected during a series of different runs at constant metal

ion concentrations and variable pH. These spectra were collected into the columns of the data matrix, **D**, which contains  $r$  rows, which indicate the spectral wavenumber dimension, and  $c$  columns, which denote the different samples at varying pH. The data matrix can be expressed as the product of the spectral and concentration behaviors of the  $n$  individual components in the sample:

$$\mathbf{D} = \mathbf{A} * \mathbf{C} \quad (1)$$

where **A** is an  $r \times n$  matrix of  $n$  pure component Raman spectra and **C** is an  $n \times c$  matrix that describes the concentration behavior of each component versus pH. The goal of this study is centered on investigating changes in concentrations of ligand forms on the silica surface; the first step of this analysis is to estimate the number of varying components that are in the data set. Malinowski [23,24] developed a test to determine the number of significant components during a run by applying a variance ratio or F test [25] to the reduced eigenvalues, REV, of the data matrix, **D**. The reduced eigenvalues are proportional to the amount of variance in the data that is described by their corresponding eigenvectors. The F ratios are obtained by a 2-way test between the first REV and the second REV, and each subsequent element of F is the 2-way test between the subsequent REV and the one after it. A large F ratio indicates that the addition of a component to the model describes significant variance in the data; the F ratios are tested for significance at the 95% confidence level to determine the number of independently varying components in the data.

Once the number of independently varying components is determined, the data matrix can be tested for the presence of component spectra of the surface-ligand, determined in advance in the absence of metal ion or in metal-ion excess, and at specific regions of pH (see below). Using these predetermined pure component spectra, **A**, a least-squares estimate of the corresponding concentration profile,  $\hat{\mathbf{C}}$ , can be found by left-multiplying the data matrix **D** by the

pseudo-inverse of the **A** matrix [26,27]:

$$\hat{\mathbf{C}} = [\mathbf{A} \mathbf{A}^T]^{-1} \mathbf{A}^T \mathbf{D} \quad (2)$$

which was evaluated using Matlab 4.2.

The concentration variation of the components is then fit to a site binding model, **C**, where the algebraic solution is evaluated using Maple version 5. The parameters in the model are varied to minimize chi-square,  $\chi^2 = (1/\sigma^2) \sum \mathbf{R}^2$ , where  $\sigma^2$  is the variance of the resolved composition profiles and  $\sum \mathbf{R}^2$  is the sum of squares of the residuals,  $\mathbf{R} = \hat{\mathbf{C}} - \mathbf{C}$ . The estimated parameter uncertainty for the optimized site-binding model were calculated by mapping the  $\chi^2$  surface within a 15% range the best fit of the parameter, *p*, and fitting the error surface to a parabola to determine its curvature. The variance in the parameter thus determined is  $\sigma_p^2 = 2/(\delta\chi^2/\delta p^2)$  [28,29]. Replicate measurements resulted in optimized parameter values that were found to lie within the uncertainty estimated from the error surface curvature.

## RESULTS AND DISCUSSION

**Raman spectra of silica-immobilized 8HQ.** Our first experiments in this study were to establish whether it would be possible to detect and distinguish the different chemical forms of the silica-immobilized 8HQ ligand in a 10 mg sample of derivatized silica packed in the micro-volume flow cell. From the surface coverages of the derivatized silica (see above), a 10 mg sample corresponds to 1.5  $\mu$ moles of the immobilized 8HQ in the flow cell. A small amount of ligand is necessary so that equilibrium can be achieved with reasonable volumes of solutions containing low concentrations of metal ion, typical of those found in trace-level metal preconcentration and analysis. The equilibration of surface ligands with low concentrations of  $\text{Cu}^{2+}$  ions in solution could be achieved with a reasonable solution volumes. For example, 100 mL of

a 30  $\mu\text{M}$   $\text{Cu}^{2+}$  solution (100% excess), loaded in 100 minutes at 1 mL/min, was more than sufficient to equilibrate the immobilized ligands, as evidenced by the Raman spectrum reaching steady-state after  $\sim 70$  mL of metal-ion solution passed through the flow cell.

The spectra of the deprotonated, protonated, neutral, and copper complexed forms of the silica-immobilized ligand were acquired and are presented in Figure 3. The deprotonated (anionic) form of the ligand was generated by equilibrating the sample with pH 10.6 phosphate buffer. The protonated form of the ligand was generated by rinsing the column with 0.10 M HCl. The neutral form of the ligand was formed by flushing the column with acetate buffer, pH=4.7; finally, the copper complex with the immobilized ligand was generated at pH = 4.7 by equilibrating the sample with 10 mM  $\text{Cu}^{2+}$ . It is clear from the resulting spectra that the protonation and metal-ion binding states of the ligand can be distinguished in the *in situ* Raman spectra. Much of the differences between these spectra arise from changes in the fractions of tautomeric forms of the ligand (see Figure 1) in response to pH and metal-ion binding [20]. The symmetric -N=N- stretching vibrations of the azo group are characterized by a strong Raman scattering in the region 1400-1450  $\text{cm}^{-1}$  due to  $\nu_{\text{N=N}}$  [30]; this band is observed at 1431  $\text{cm}^{-1}$  for the anion and copper-complex form of the ligand. The two bands at 1141 and 1196  $\text{cm}^{-1}$  for the anion and complexed ligand correspond to the C-N azo symmetric stretch, and C-N azo symmetric bend, respectively. The frequencies of these three bands are identical to the uncomplexed azo-quinoline species [30] which indicates that the metal ion coordination does not involve N-atoms in the azo bridge but the stronger N,O-sites of the quinoline ring. The 1141 and 1431  $\text{cm}^{-1}$  C-N azo bands are also observed in the neutral form of the ligand at smaller intensities when compared to the anion and complexed form. The protonated form has an even more diminished 1141  $\text{cm}^{-1}$  band, and its  $\nu_{\text{N=N}}$  band at 1431  $\text{cm}^{-1}$  appears only as a shoulder. The intense peak at 1378  $\text{cm}^{-1}$  is strong in the metal ion complex form of the ligand; this band is due to the  $\nu_{\text{C-C}}$

mode of the quinoline ring [31] and appears as a shoulder in the neutral and deprotonated forms of the ligand.

The decrease in the intensities of both of the azo and quinoline bands for the protonated and neutral forms of the ligand is consistent with formation of a hydrazone tautomer [30,31]. The large band at  $1590\text{ cm}^{-1}$  corresponds to the  $\nu_{\text{C}=\text{C}}$  stretching vibrations of the phenol ring, and the peak intensity of this band for the uncomplexed ligand forms is strong, consistent with hydrazone formation [31]. Further evidence of the presence of this tautomer is the shoulder at  $\sim 1620\text{ cm}^{-1}$  which has been assigned to  $\nu_{\text{C}=\text{N}}$  and  $\nu_{\text{C}=\text{O}}$  in hydrazones of azonaphthols and azoquinolines [30]. Other evidence of this tautomer for both the protonated and neutral ligands is the  $1283\text{ cm}^{-1}$   $\nu_{\text{C}-\text{C}}$  in-plane stretching band that is associated with the hydrazone form of the ligand. The observed spectrum show that the protonated ligand is predominately in the hydrazone form, the neutral and anion ligand exists in both tautomers (the anion exhibiting more azo-quinoline character), and the metal-complexed ligands are predominately in the azo form. Deprotonation at high pH drives the ligand toward the azo form to favor phenoxide anion formation on the more electronegative oxygen over an azide ion by loss of hydrogen ion from the nitrogen linker portion of the molecule. The spectra of the metal ion complex are consistent with metal-ion binding to the phenoxide anion formed from the azo tautomer of the ligand, which also allows interactions with the nitrogen in the quinoline ring.

**Interfacial metal-ion complexation and surface potential.** Free-solution complexation of 8HQ with metal ions generally exhibits a stoichiometry that is the same as the metal ion charge [11]. For example,  $\text{Cu}^{2+}$ , forms a binary 8HQ complex in free solution with formation constants  $10^{12}$  and  $10^{11}$  for binding the first and second ligand, respectively [11,32]. One difference between solution-phase and silica-bound ligands is their ability to form higher-order complexes. At low surface coverages, immobilized ligands may be spaced too far apart to allow

formation of higher order complexes, so that the complexation ratio of metals to silica-immobilized 8HQ is limited to 1:1 [20]. A second difference in interfacial metal-ion complexation is that the reaction takes place in a different chemical environment than bulk solution due to the surface potential of the silica, which will alter the chemical potential of ions in the vicinity of the surface [14-19]. The silica gel itself exhibits a surface charge due to deprotonation of silanols, and non-specific adsorption of other ions from solution to the silica surface can alter the potential.

The surface potential may affect the reactivity of a surface ligand since ion activities near the surface will be altered from their bulk solution values due to the surface potential. Since the binding site of immobilized 8HQ is tethered by a relatively stiff linkage well away from the silica surface, the complexation reaction takes place beyond the Stern layer of strongly adsorbed ions in the diffuse layer of solution phase ions; the ion densities present in this region can be modeled by Gouy-Chapman theory [33]. The relationship between the activity of cations at a distance  $x$  away from the charged surface ( $\bar{a}_{i,x}$ ) and in bulk solution ( $a_i$ ) is given by the Boltzmann equation:

$$\bar{a}_{i,x} = a_i * \exp\left(\frac{-zF\psi_x}{RT}\right) \quad (3)$$

where  $\psi_x$  is the potential at a distance  $x$  away from the charged surface,  $z$  is the charge on the ion,  $F$  is Faraday's constant,  $R$  is the gas constant, and  $T$  is the absolute temperature of the solution. The Boltzmann relationship is only strictly true for ion densities expressed as activities; however, the relationship is routinely applied to concentrations when the concentrations are small [33].

The binding of  $\text{Cu}^{2+}$  due to complexation by the immobilized 8HQ thus depends on the electrical potential of the silica surface, and its effect on cation exchange in the diffuse part of

the electrical double layer. The surface potential of the silica arises primarily from protonation and deprotonation of silanol groups [34] and from the adsorption and binding of metal ions at the silica surface [14,16,18,22]. To understand and model the effect of surface potential on interfacial complexation reactions by immobilized 8HQ, we measured the  $\zeta$  potential of the derivatized silica for several different pH solutions containing three different  $\text{Cu}^{2+}$  concentrations to span the range of spectroscopic studies.

The  $\zeta$  potential of the 8HQ-silica for each of the solution conditions is plotted in Figure 4. When no  $\text{Cu}^{2+}$  is present in solution, the  $\zeta$  potential is negative for all solutions above a pH of 2.7 due to deprotonation of silanol groups; at a pH < 2.7, protonation of surface silanols leads to a weakly positive surface. The isoelectric pH of  $2.7 \pm 0.2$  for the 8HQ-derivatized silica agrees with previous  $\zeta$ -potential measurements made on bare silica [34-36]. This is not surprising since the surface concentration of 8HQ ligands is small and their neutral form is dominant at the isoelectric pH of the silica surface. At higher pH values, the  $\zeta$  potential values are less negative than for bare silica under similar conditions [36]; the difference could be due to the silica-immobilized 8HQ shifting the position of the shear plane away from the particle surface or influencing the degree of silanol deprotonation by changing the interfacial dielectric constant. The addition of  $\text{Cu}^{2+}$  to solution changes the silica surface potential to positive values, with an effect that increases for higher metal ion concentrations. The effect of  $\text{Cu}^{2+}$  on the  $\zeta$  potential persists at pH values less than 2.5, where binding of the metal ion to immobilized 8HQ is negligible (see below). This result indicates that the effect of  $\text{Cu}^{2+}$  on the silica surface potential is not only due to its binding to 8HQ ligands, but also due to adsorption to the silica surface which has a large population of surface silanols capable of interacting with transition metal ions from solution.

The effect of surface potential on an interfacial reaction with a tethered ligand depends

on the distance at which the reaction occurs away from the charged surface. The  $\zeta$  potential is measured at the plane of shear between strongly adsorbed, potential-determining ions and bulk solution, which is very close to the outer-Helmholtz plane at the centers of the counterion layer. Based on radii of the ions in the double layer [37], this plane will be approximately 4 - 6 Å away from the surface silanols. For silica-immobilized 8HQ, proton-transfer and metal-ion binding reactions take place at the outer surface of the quinoline ring, which is held by a rigid linkage ~ 8 Å away from the silica silanol binding site [38]. Thus, reactions of the immobilized ligand take place approximately 3 Å beyond the shear plane where the  $\zeta$  potential is measured. The interfacial potential where reaction occurs,  $\psi_x$ , will be proportional to the  $\zeta$  potential corrected by decay in the diffuse double layer:  $\psi_x = \zeta \exp(-\kappa \Delta x)$ , where  $\Delta x \sim 3$  Å and  $\kappa$  is the inverse Debye length,  $\kappa = [e^2 \sum n_i z_i^2 / \xi kT]^{1/2}$ , which is  $\sim 0.096$  Å<sup>-1</sup> for our ionic strength conditions of 100 mM. The decay of the diffuse double layer predicts that  $\psi_x \sim 0.75 \zeta$ , which allows the measured values of the zeta potential to be used in Equation 3 to correct bulk ion activities for the effect of the potential at the interface.

**Acid-base chemistry of immobilized 8HQ.** Insight into the reactivity of the immobilized ligand on the silica surface can be gleaned by investigating the equilibrium for the metal-ion binding reaction:



The equilibrium constant for this reaction,  $K^0$ , is strongly influenced by pH since the activity of the anion form of the ligand varies with pH. The anion form of the ligand dominates above a pH of 8 [19], while below a pH ~ 3 or 4 [9,18] the ligand is protonated. At intermediate pH values, the neutral form of the ligand dominates. In homogeneous aqueous solutions, 5-(p-phenylazo)-8-quinolinol HCl exhibits a  $\text{pK}_{\text{A}1}$  of 3.2 for the dissociation of the protonated ligand to form a

neutral species [39]. Different substituents at the ortho, meta, and para positions of the phenylazo group do not change the dissociation values by more than  $\pm 0.8$  pH units, unless the group is highly electron withdrawing [39]. Thus, by analogy with homogeneous aqueous solution behavior, the silica-immobilized 8HQ should have a first acid dissociation constant in the range of 2.4 - 4.0. Previous acid-base titrations have been conducted on silica-immobilized 8HQ and resulted in values of 3.3-3.8 [9]. However, bare silica gel was also observed to yield similar  $pK_A$  values, which indicates that these values could be influenced by the titration of the silanol groups on the silica surface [9].

These previously reported values for the first acid dissociation constant of silica-immobilized 8HQ did not use *in-situ* detection methods to directly observe the pH dependence of the acid-base forms of the ligand. Since Raman spectroscopy allows the direct observation and discrimination of the forms of the ligand (see Figure 3 and discussion, above), it provides a potent tool for investigating the interfacial reactions of this ligand. Buffered solutions of known pH and constant ionic strength (0.1 M) were flowed through the micro-column for 30 minutes at 1 ml/min, and then a Raman spectrum of the surface-bound ligand was obtained for each of these pH conditions (Figure 5). The pH-dependent changes in the band intensities can be observed in the surface-plot of these spectra, where scattering from the protonated form of the ligand decay with increasing pH, while bands from the neutral form rise with increasing pH. The  $pK_{A1}$  can be determined by fitting the relative concentrations (obtained from their Raman scattering, neglecting changes in activity coefficients of the ligand with pH) for the protonated and neutral forms of the ligand during the titration. Using normalized pure component spectra of the protonated and neutral form of the ligand (see above), a multidimensional least squares analysis (Equation 2) was used to determine the relative concentrations of each species versus pH, and the results are plotted in Figure 6.

To fit the data in Figure 6 to determine the first acid dissociation constant from changes

in composition with pH, we first utilize a conservation of mass expression for the two forms of the ligand (whose amplitudes are normalized):

$$[HQH^+] = 1 - [HQ] \quad (5)$$

combined with the equilibrium expression for their ratio:

$$\frac{[HQ]}{[HQH^+]} = \frac{K_{A1}}{a_H \exp\left(\frac{-F\Psi_x}{RT}\right)} \quad (6)$$

where the proton activity in solution,  $a_H$ , is modified at the interface by the Boltzmann equation depending on the surface potential, which is known from the  $\zeta$  potential measurements (see above). These two expressions are solved for HQ and  $HQH^+$  for a series of acid dissociation constants,  $K_{A1}$ , and the least-squares best fit to the pH-dependent concentration profiles (over the pH range where the surface potential is known) is found for  $pK_{A1} = 2.7 \pm 0.1$ . The quality of fit of the ligand concentration data to the interfacial proton-transfer equilibrium model adds confidence that the results are reporting the reaction of the silica-immobilized 8HQ and not the titration of the hydroxyl groups on the silica surface, although titration of surface silanols is implicitly included in the model through their effect on the surface potential over this range of pH.

The second acid dissociation step of 8HQ is crucial in defining the activity of the anion form of the ligand versus pH. Previous *in situ* absorbance measurements conducted through a thin layer of 8HQ immobilized onto controlled pore glass were used to determine the second acid dissociation constant,  $pK_{A2} = 8.6$  [19]. This work also reported that the measured  $pK_{A2}$  was insensitive to surface potential, where a more flexible propyl amine used to attach 5-(phenyl-azo)-8-hydroxyquinoline onto the surface allowed the distance between the charged surface

and 8HQ to increase with increasing pH. To determine the second acid dissociation constant for the more rigid phenylazo-linked 8HQ, we measured the Raman scattering from the neutral and deprotonated forms of the ligand over a pH range from 6.1 to 10.6 at a constant ionic strength of 0.1 M. Note, these measurements were made using a larger volume flow cell [20] containing ~300 mg of derivatized silica to increase the sensitivity of the measurement for resolving the anionic and neutral forms of the ligand since their spectra are quite similar. The larger amount of sample is not critical for acid-base experiments since the buffer concentration is high (50 mM), which can equilibrate the ligand and surface silanols with a reasonable volume (30 mL) of solution. Using the predetermined pure component spectrum, a least squares analysis (Equation 2) was used to determine the concentration profiles for both the neutral and anionic form of the immobilized ligand versus pH. The results are plotted in Figure 7, along with the least-squares best fit concentration profiles of the neutral and anionic forms of the ligand from the following two equations.

$$[HQ] = 1 - [Q^-] \quad (7)$$

and

$$\frac{[Q^-]}{[HQ]} = \frac{K_{A2}}{a_H \exp\left(\frac{-F\Psi_x}{RT}\right)} \quad (8)$$

where the measured  $\zeta$  potentials are again used to estimate the surface potential in Equation 8. The best-fit expressions resulted in a  $pK_{A2}$  of  $8.6 \pm 0.25$ , which is within errors for the value determined spectroscopically for the ligand bound with a more flexible tether to a CPG surface [19]. By including the surface-potential influence in the analysis of the more rigid, phenyl-azo linked ligand, the intrinsic proton-transfer chemistry of the immobilized 8HQ forms are found to

be comparable.

**Metal-ion binding by immobilized 8HQ.** Given the above measured values for the proton-transfer equilibrium constants for immobilized 8HQ, the  $\text{Cu}^{2+}$  binding reaction by the ligand can be investigated by observing the pH dependence of the complexation equilibria through monitoring the concentration profiles of the bound and free ligand. Buffered solutions at a constant ionic strength of 0.1 M containing 5 mM, 600  $\mu\text{M}$  and 30  $\mu\text{M}$   $\text{Cu}^{2+}$  were pumped through the sample column at 1 ml/min for 30 min, 40 min, and 100 min, respectively. The high binding capacity of the immobilized silica (0.15 mmol/g) requires that the mass of the packing in the micro column to be small ( $\sim 10$  mg) corresponded to 1.5  $\mu\text{mol}$  of 8HQ. During experiments with 30  $\mu\text{M}$   $\text{Cu}^{2+}$ , the column was flushed with twice as many moles of  $\text{Cu}^{2+}$  as there were immobilized 8HQ ligands, and the spectra did not change following exposure of the sample to additional metal ion; previous studies showed that exposure to only  $\sim 30\%$  excess metal ion are required for the sample to reach equilibrium [20].

For each  $\text{Cu}^{2+}$  concentration, Raman spectra were obtained as a function of pH to observe the complexation reaction and determine the speciation of the sample. An example is shown in Figure 8 for the pH dependence of metal-ion binding for a solution containing 5 mM  $\text{Cu}^{2+}$ . In the higher pH region of the data, bands of the metal-complex increase and dominate the spectra, while bands from the protonated form of the ligand decay away. At the high metal ion concentration, the neutral form of the ligand is difficult to identify in the data since its concentration is relatively low (see below). Nevertheless, the number of significant components in the data of Figure 8 was determined by factor analysis [23] to be 3 which should correspond in this pH range to the protonated, neutral, and complexed forms of the ligand. Using the component spectra corresponding to these three forms of the ligands, a least-squares analysis of the component concentrations was performed using Equation 2. Figure 9A shows the resulting pH-dependent concentration profiles of the protonated, neutral, and complexed forms

of the ligand for solutions containing 5 mM  $\text{Cu}^{2+}$ . Figures 9B and C show similar results for 600  $\mu\text{M}$  and 30  $\mu\text{M}$   $\text{Cu}^{2+}$  solutions, respectively. At lower metal ion concentrations, the pH must be higher in order to observe the complexed form of the ligand; at higher pH, the activity of the anionic,  $\text{Q}^-$ , is increased favoring the binding of the ligand to metal ion. At lower metal ion concentrations, one can also observe the appearance of the neutral form of the ligand at higher pH prior to the appearance of the metal-ion complex.

To understand the interfacial metal-ion complexation equilibria that are governing these results, the concentration profiles were fit to a site-binding equilibrium model that includes the two acid-base equilibria represented in Equations 6 and 8 and their respective acid dissociation constants, determined above. The mass balance expression for the normalized ligand concentration is given by:

$$[\text{CuQ}^+] = 1 - [\text{Q}^-] - [\text{HQ}] - [\text{HQH}^+] \quad (9)$$

while the fraction of the metal complex formed in the reaction of Equation 4 is given by the equilibrium expression:

$$\frac{[\text{CuQ}^+]}{[\text{Q}^-]} = K^o [\text{Cu}^{2+}] \exp\left(\frac{-2 F \Psi_x}{RT}\right) \quad (10)$$

where the activity of  $\text{Cu}^{2+}$  in the double-layer is modified by the exponential term from the Boltzmann equation. The values of the  $\zeta$  potential for the 8HQ silica measured in the presence of  $\text{Cu}^{2+}$  (Figure 3, inset) are used to estimate the surface potential,  $\Psi_x \sim 0.75 \zeta$  (see above), in Equations 6, 8, and 10. These three expressions together with the mass balance for the ligand (Equation 9) were solved numerically for a range of equilibrium constants,  $K^o$ , and the results were tested for their fit to the measured concentration profiles in Figure 9, over the pH range

where the  $\zeta$  potential was measured.

The best fit values of the equilibrium constant were consistent for the 3 different metal ion concentrations, where  $K^O = 4.75 (\pm 0.2) \times 10^8$  for  $[\text{Cu}^{2+}] = 5 \text{ mM}$ ,  $K^O = 4.65 (\pm 0.2) \times 10^8$  for  $[\text{Cu}^{2+}] = 600 \text{ }\mu\text{M}$ , and  $K^O = 4.8 (\pm 0.2) \times 10^8$  for  $[\text{Cu}^{2+}] = 30 \text{ }\mu\text{M}$ . The consistent values of  $K^O$ , which are indistinguishable within their uncertainties, provide strong evidence that the surface potential corrections to the interfacial ion activities, derived from the measured  $\zeta$  potentials, are valid and useful for obtaining information about the reactivity of the immobilized ligand. Neglecting this correction leads to large (two-fold) changes in the apparent metal-ion binding constant over the range of  $[\text{Cu}^{2+}]$  in these data, where the apparent binding constant decreases at higher  $\text{Cu}^{2+}$  concentrations due to the more positive surface potential. Correcting for the interfacial ion activities for this effect leads to a single value of the metal-ion binding equilibrium constant, independent of metal ion concentration.

The value of  $K^O$  for  $\text{Cu}^{2+}$  binding to silica-immobilized 8HQ ligands can be compared to the first binding step for a comparable ligand in free solution. We recently investigated [40] a water soluble 8HQ ligand [39]: 5-(p-sulfophenylazo)-8-hydroxyquinoline, where a sulfonic-acid group is substituted for the siloxane linkage on our immobilized ligand. This ligand includes the phenylazo structure bound to the 5-position on the quinoline ring, so that effects of ligand tautomerism are preserved. Using very low concentrations of this ligand in solution compared to the copper ion concentration, the equilibrium constant for the first ligand binding step could be measured by absorption spectroscopy in the visible region [40]; the resulting equilibrium constant is  $3.1 \times 10^{10}$ , or about 60-times greater than a comparable ligand on the silica surface. The lower reactivity of the immobilized ligand could be due to several factors, including loss of adsorption interactions between the ligand and the silica surface or conformational mobility upon  $\text{Cu}^{2+}$  binding due to charge repulsion or greater stability of the zwitterionic complex in

solution (the sulfonic acid is deprotonated at the pH conditions of the reaction) compared to the cationic complex on the positively charged surface. Further research to address these issues, including studies of solvent effects that can influence ligand adsorption and independent control of the surface potential via SERS-based spectroelectrochemistry, is in progress.

### **ACKNOWLEDGMENTS**

This research was supported in part by a grant from the U.S. Department of Energy (DE-FG03-93ER14333). The authors would also like to thank Jakub W. Nalaskowski for his assistance in obtaining the  $\zeta$ -potential measurements.

**REFERENCES**

1. Bruening, R. L.; Tarbet, B. J.; Krakowiak, K. E.; Bruening, M. L.; Izatt R. M.; Bradshaw, J. S. *Anal. Chem.* **1991**, 63, 1014-1017.
2. Izatt, R. M.; Pawlak, K.; Bradshaw, J. S.; Bruening, R. L.; *Chem. Rev.* **1991**, 91, 1721-1785.
3. Jezorek, J. R.; Tang, J.; Cook, W. L.; Obie, R.; Ji, D.; Rowe, J. M. *Anal. Chim. Acta* **1994**, 290, 303-315.
4. Lessi, P.; Moreira, J. C.; Filho, N. L.; Campos, J. T. *Anal. Chim. Acta* **1996**, 327, 183.
5. Hankins, M. G.; Hayashita, T.; Kasprzyk, S. P.; Bartsch, R. A. *Anal. Chem.* **1996**, 68, 2811-2817.
6. Feng, X.; Fryxell, G. E.; Wang, L.-Q.; Kim, A. Y.; Liu, J.; Kemner, K. M. *Science* **1997**, 276, 923-926.
7. Hill, J. M. *J. Chromatogr.* **1973**, 76, 455-458.
8. Jezorek, J. R.; Freiser, H. *Anal. Chem.* **1979**, 51, 366-373.
9. Marshall, M. A.; Mottola, H. A. *Anal. Chem.* **1983**, 55, 2089-2093.
10. Marshall, M. A.; Mottola, H. A. *Anal. Chem.* **1985**, 57, 729-733.
11. Starý, J.; Zolotov, Y. A.; Petrukhin O. M. *Critical Evaluation of Equilibrium Constants Involving 8-Hydroxyquinoline and its Metal Chelates*; IUPAC Chemical Data Series No 24; Pergamon Press: Oxford, U.K., **1979**.
12. Sturgeon, R. E.; Berman, S. S.; Willie, S. N.; Desaulniers, J. A. H. *Anal. Chem.* **1981**, 53, 2337-2340.
13. Bernal, J. P.; Rodriguez De San Miguel, E.; Aguilar, J. C.; Salazar, G. De Gyves, J. *Sep. Sci. Technol.* **2000**, 35, 1661-1679.
14. Vermeulen, D. M.; Cantwell, F. F. *Anal. Chem.* **1993**, 65, 1360-1366.

15. Chow, P. Y. T.; Cantwell, F. F. *Anal. Chem.* **1988**, 60, 1569-1573.
16. Vermeulen, D. M.; Cantwell, F. F. *J. Chromatogr. A* **1995**, 693, 205-216.
17. Howard, M. E.; Holcombe, J. A. *Anal. Chem.* **2000**, 72, 3927-3933.
18. Weaver, M. R.; Harris, J. M. *Anal. Chem.* **1989**, 61, 1001-1010.
19. Kolstad, K.; Chow, P. Y. T.; Cantwell, F. F. *Anal. Chem.* **1988**, 60, 1565-1569.
20. Uibel, R. H.; Harris, J. M. *Appl. Spec.* 2000, 54, 1868-1875.
21. Benyon, R. J.; Easterby, J. S. *Buffer solutions The Basics*; IRL Press; Oxford, **1996**.
22. Hunter, R. J. *Zeta Potential in Colloid Science: Principles and Applications*; Academic Press; New York; New York, **1981**.
23. Malinowski, E. R. *Factor Analysis in Chemistry*, 2<sup>nd</sup> ed.; John Wiley and Sons; New York, **1991**.
24. Malinowski, E. R. *Anal. Chem.* **1977**, 49, 612-617.
25. Barlow, R. J. *Statistics a Guide to the Use of Statistical Methods in the Physical Sciences*, John Wiley and Sons; New York, New York, **1989**.
26. Draper, N. R.; Smith, H. *Applied Regression Analysis*; John Wiley and Sons; New York, New York, **1981**.
27. Tauler, R.; Kowalski, B.; Fleming, S. *Anal. Chem.* **1993**, 65, 2040-2047.
28. Bevington, P. R. *Data Reduction and Error Analysis for the Physical Sciences*; McGraw-Hill Book Co.; New York, New York, **1969**.
29. Phillips, G. R.; Eyring, E. M. *Anal. Chem.* **1988**, 60, 738-741.
30. Trotter, P. J. *Appl. Spectrosc.* **1977**, 31, 30-35.
31. Bajpai, P. K.; Pal, B.; Baul, T. S. B. *J. Raman Spectrosc.* **1995** 26, 351-361.
32. Starý, J. *Anal. Chem. Acta.* **1963**, 28, 132-149.

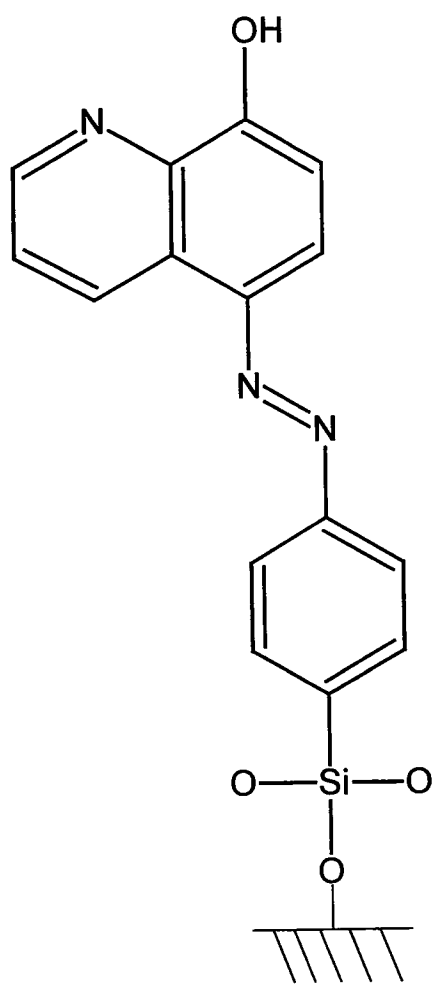
33. Adamson, A. W. *Physical Chemistry of Surfaces*, 4<sup>th</sup> ed.; John Wiley and sons; New York; New York, **1982**.
34. Healey, T. W.; White, L. R. *Adv. Colloid Interface Sci.* **1978**, 9, 303-345.
35. Scales, P. J.; Grieser, F.; Healy, T. W.; White, L. R.; Chan, D. Y. C. *Langmuir* **1992**, 8, 965-974.
36. Hartley, P. G.; Larson, I.; Scales, P. J.; *Langmuir* **1997**, 13, 2207-2214.
37. Dean, J. A., *Lange's Handbook of Chemistry*, McGraw-Hill: New York, **1992**; Section 8.
38. Note: this assumes 8HQ binding to two surface silanols producing a tilt angle of phenyl-azo linker by  $\sim 50^\circ$  from the surface normal.
39. Khater, M. M.; Issa, Y. M.; Shoukry, A. F. *J. Prakt. Chemie.* **1980**, 322, 470-474.
40. Uibel, R. H.; Harris, J. M. unpublished results, manuscript in preparation.

**FIGURE CAPTIONS**

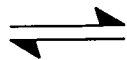
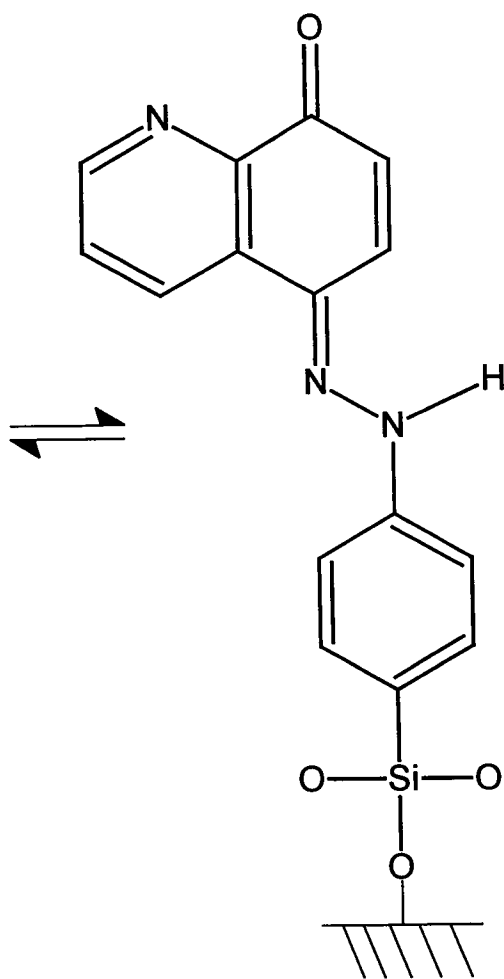
1. Structure of the silica-immobilized 8HQ, showing the two tautomeric forms of the ligand.
2. *In-Situ* Raman spectroscopy instrument used to monitor metal-ion complexation to silica immobilized 8HQ. See text for description.
3. Normalized Raman spectra of silica-immobilized 8HQ: deprotonated (top), protonated (2nd down), neutral (3rd down), and complexed to  $\text{Cu}^{2+}$  (bottom).
4. Zeta potential of the silica-immobilized 8HQ. Full plot are results without  $\text{Cu}^{2+}$  in solution. The inset plot shows the zeta potential of solutions containing the  $\text{Cu}^{2+}$  at 5mM (top), 600  $\mu\text{M}$  (middle), and 30  $\mu\text{M}$  (bottom).
5. Normalized Raman spectra of silica-immobilized 8HQ over a pH range of 1.30 to 4.49, showing the titration of the protonated to neutral forms of the ligand. No  $\text{Cu}^{2+}$  is present in solution.
6. Relative concentrations of silica-immobilized 8HQ in its protonated (squares) and neutral (circles) forms determined from the Raman spectra of Figure 5. The data are fitted to Equations 5 and 6 (full line) over the pH range where the  $\zeta$  potential was measured (Figure 4).
7. Relative concentrations of silica-immobilized 8HQ in its neutral (circles) and anionic (plus) forms. The data are fitted to Equations 7 and 8 (full line) using the measured surface potential data from Figure 4.
8. Normalized Raman spectra of silica-immobilized 8HQ over a pH range of 1.5 to 4.5 with 5mM  $\text{Cu}^{2+}$  in solution.

9. Relative concentrations of silica-immobilized 8HQ in its protonated (squares), neutral (plus) and  $\text{Cu}^{2+}$ -complex forms (circles), in equilibrium with solutions containing 5mM, 600  $\mu\text{M}$ , and 30  $\mu\text{M}$   $\text{Cu}^{2+}$  for panels A, B, and C, respectively. The data are fitted to Equations 9 and 10 (full line) over a pH range where the  $\zeta$  potential was measured (Figure 4 (inset)), with the pH-dependent activity of  $\text{Q}^-$  determined from Equations 6 and 8 using the previously measured values of the  $\text{pK}_{\text{A}1}$  and  $\text{pK}_{\text{A}2}$ .

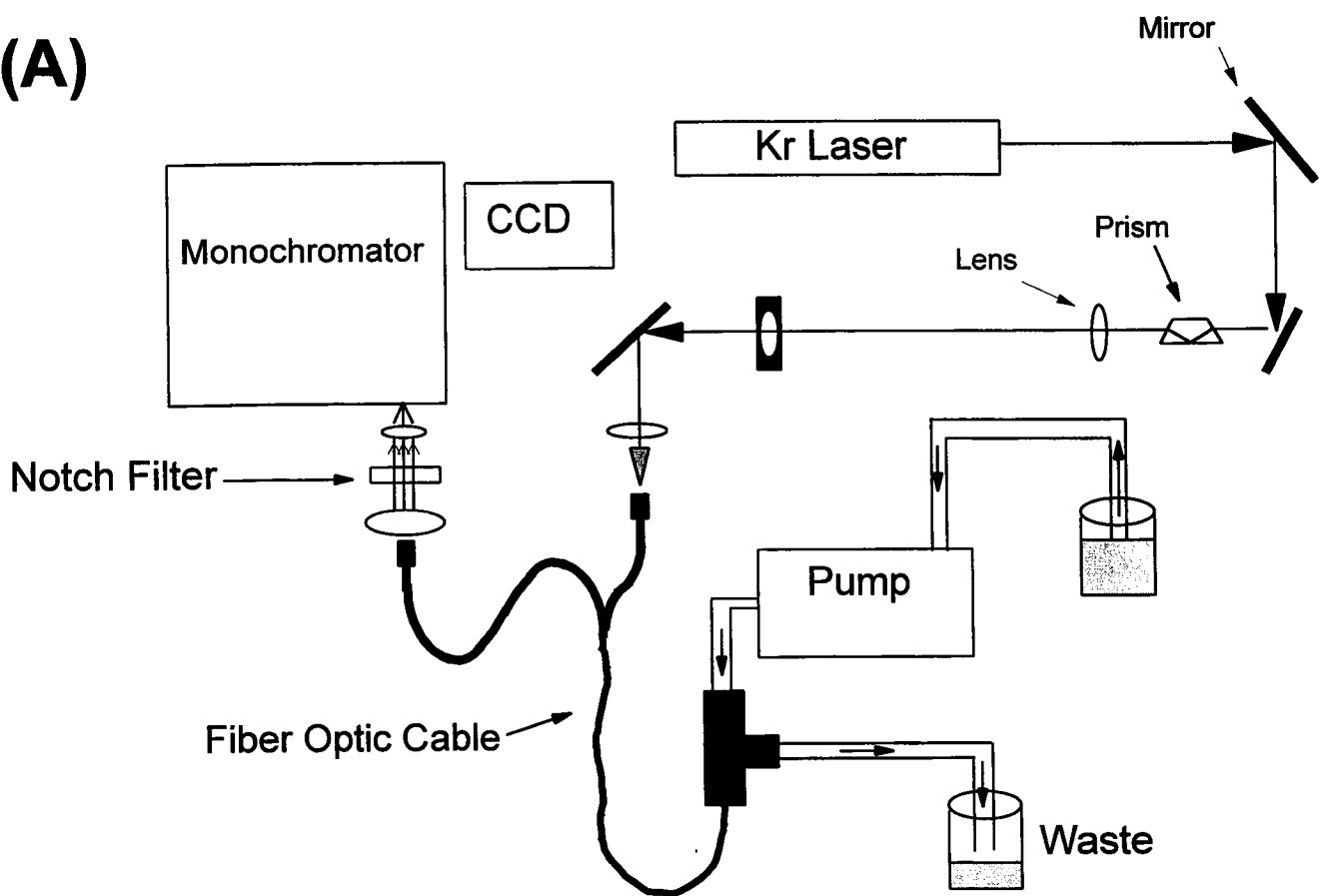
Azo Form



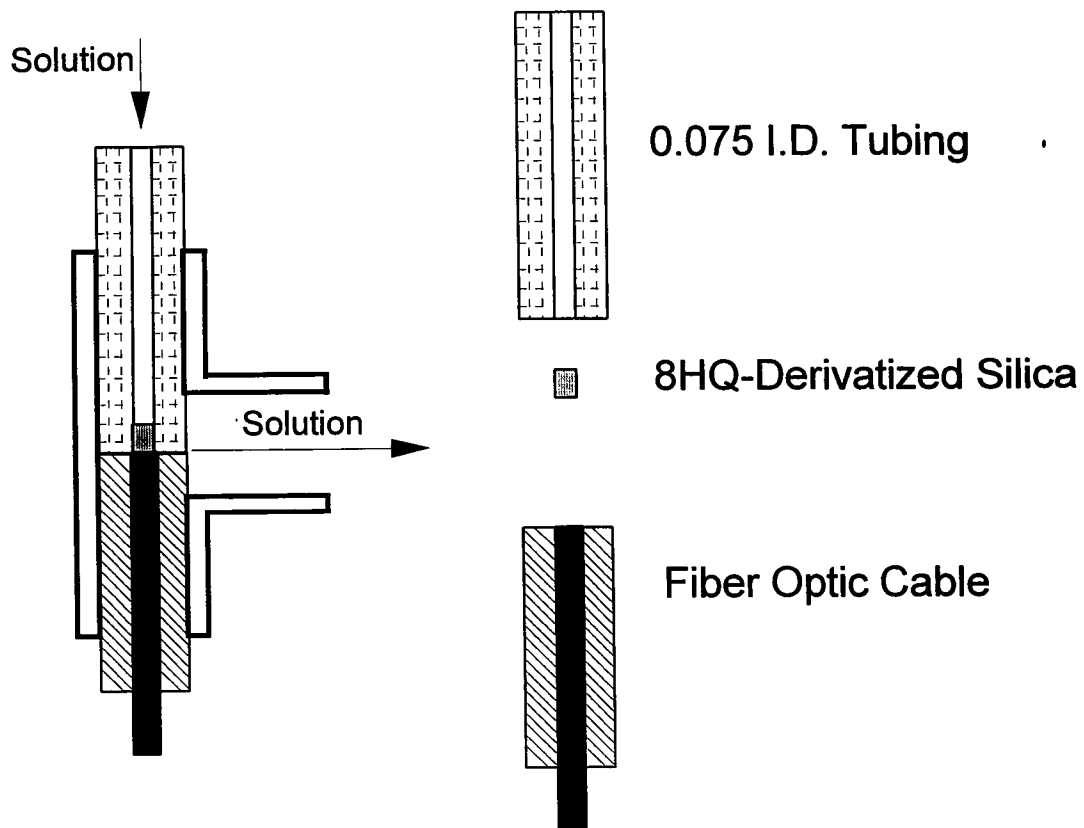
Hydrazone Form

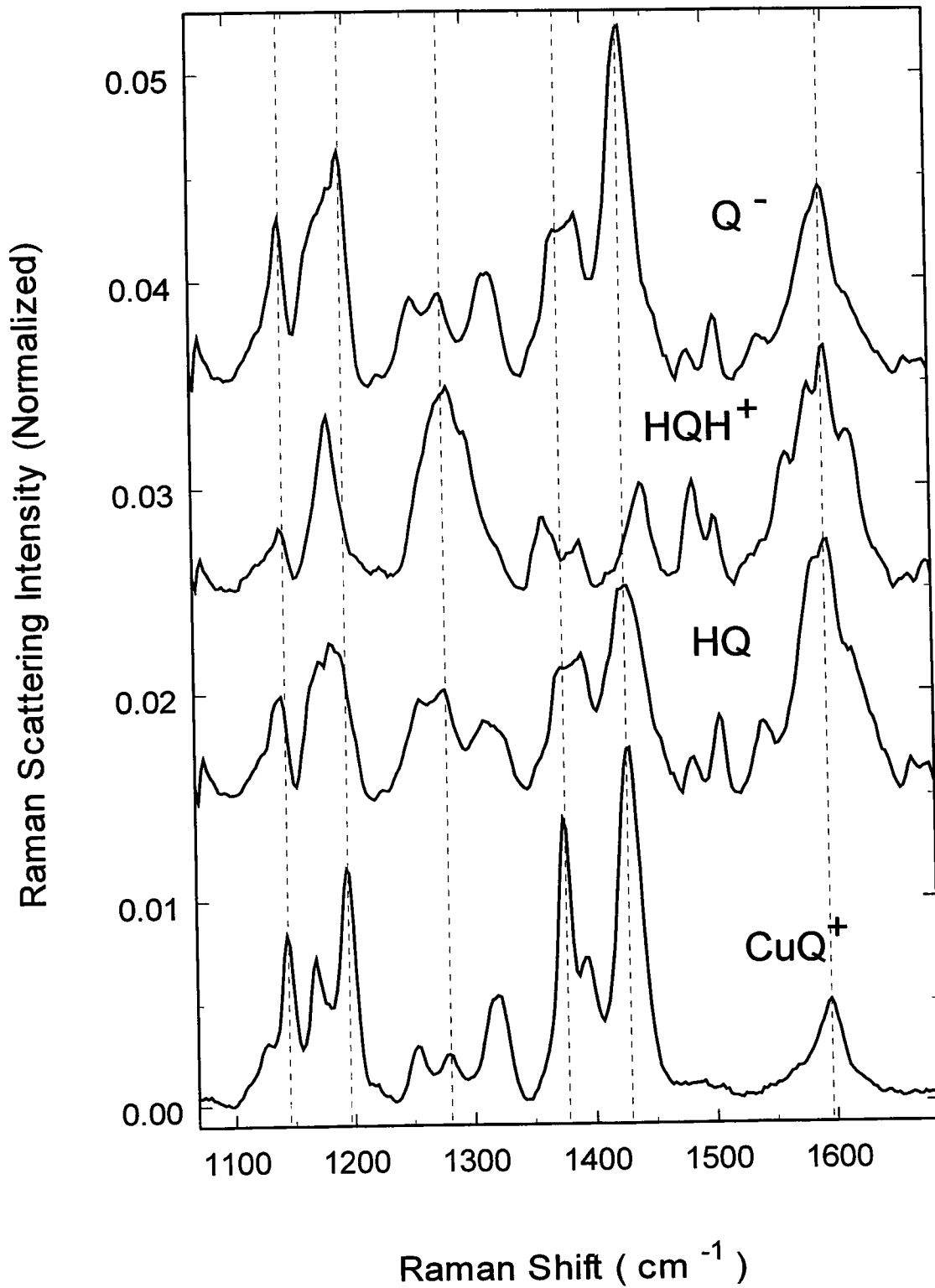


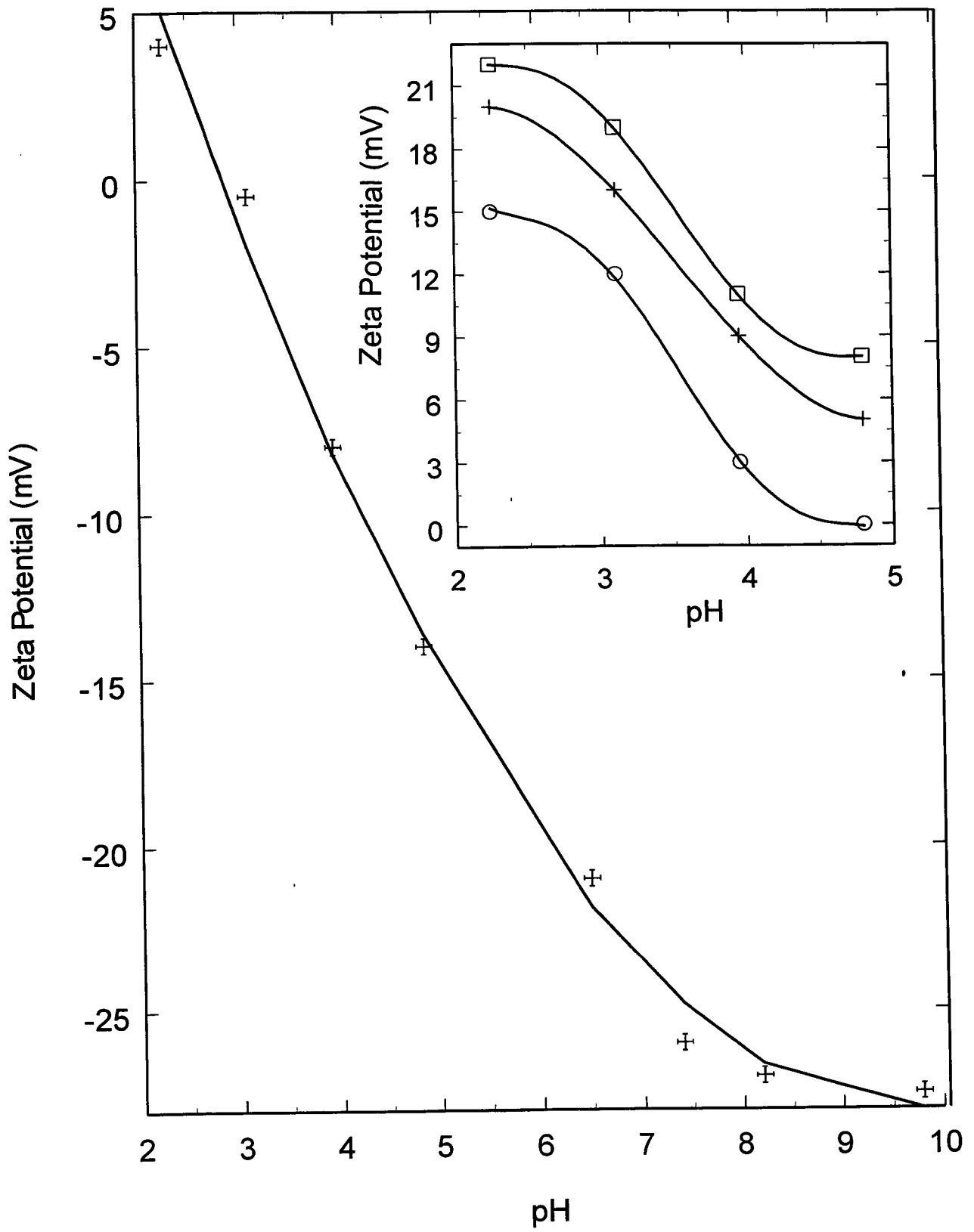
**(A)**

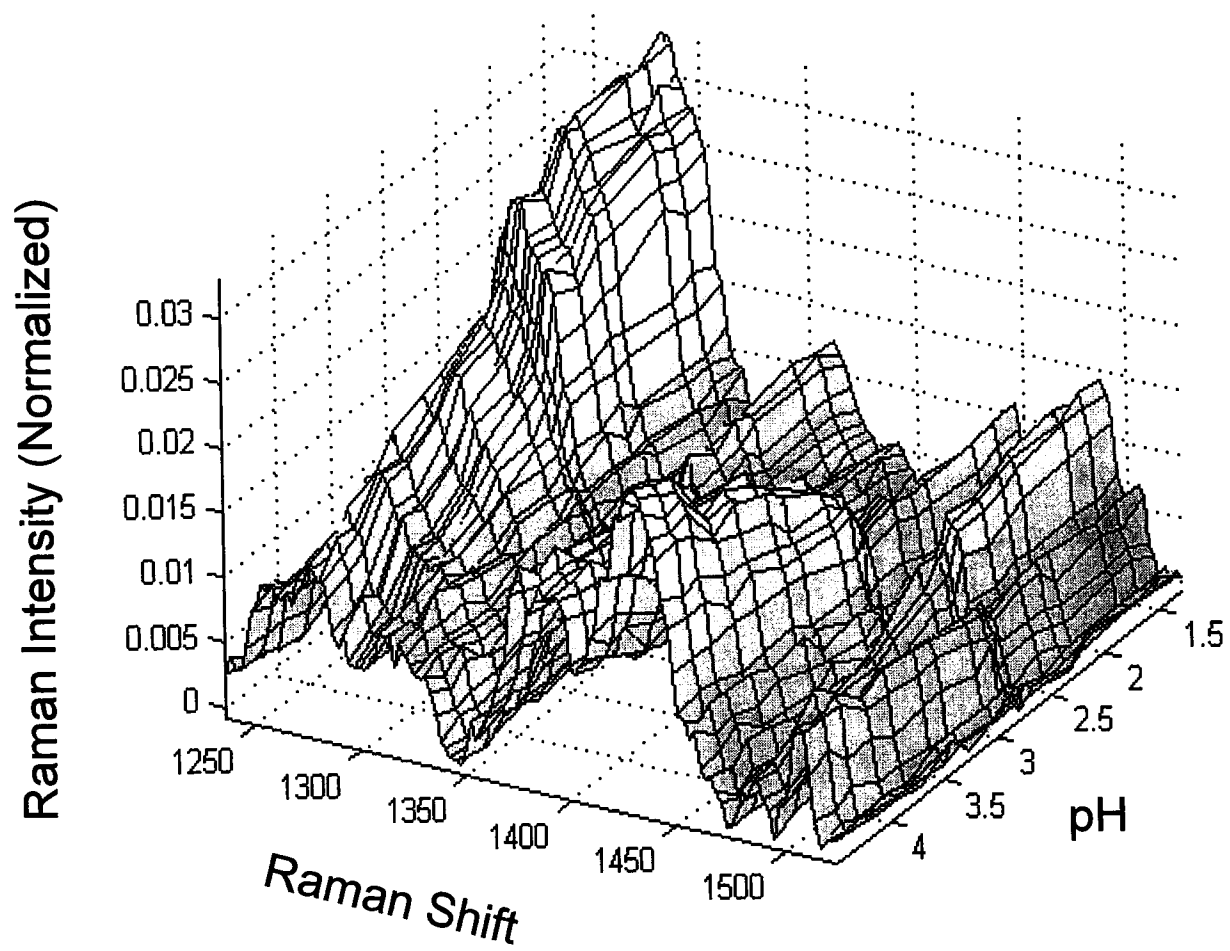


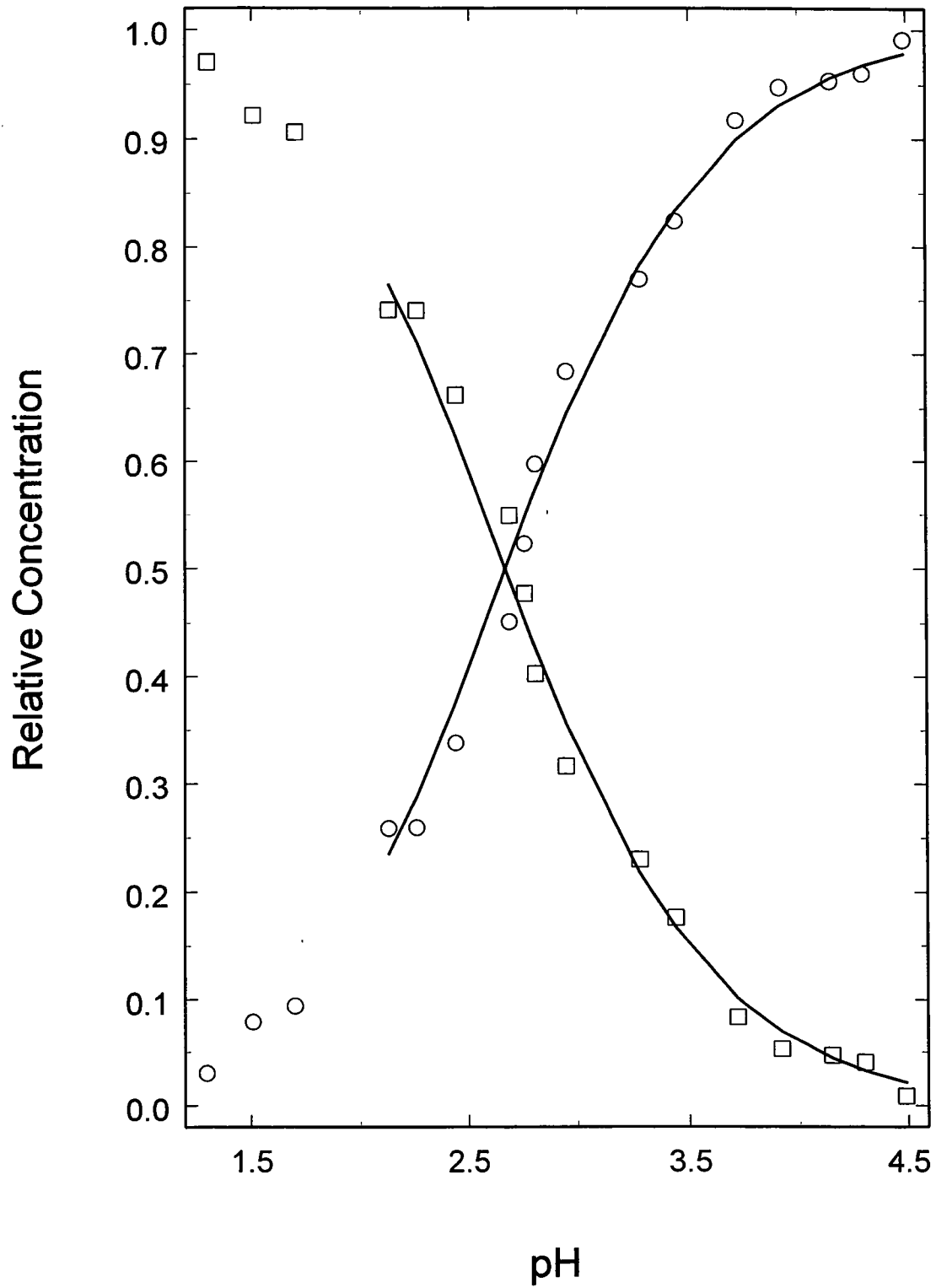
**(B)**

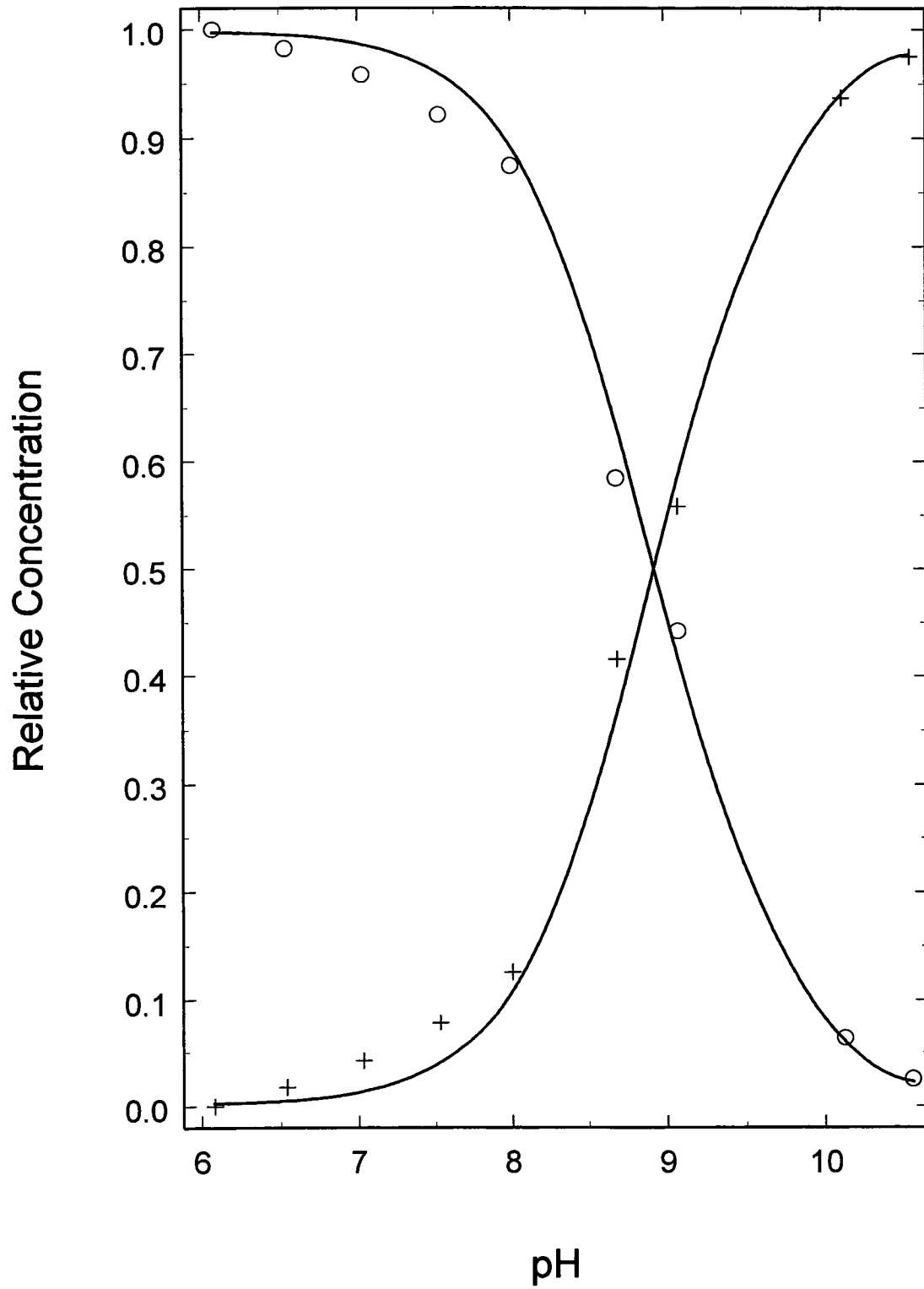


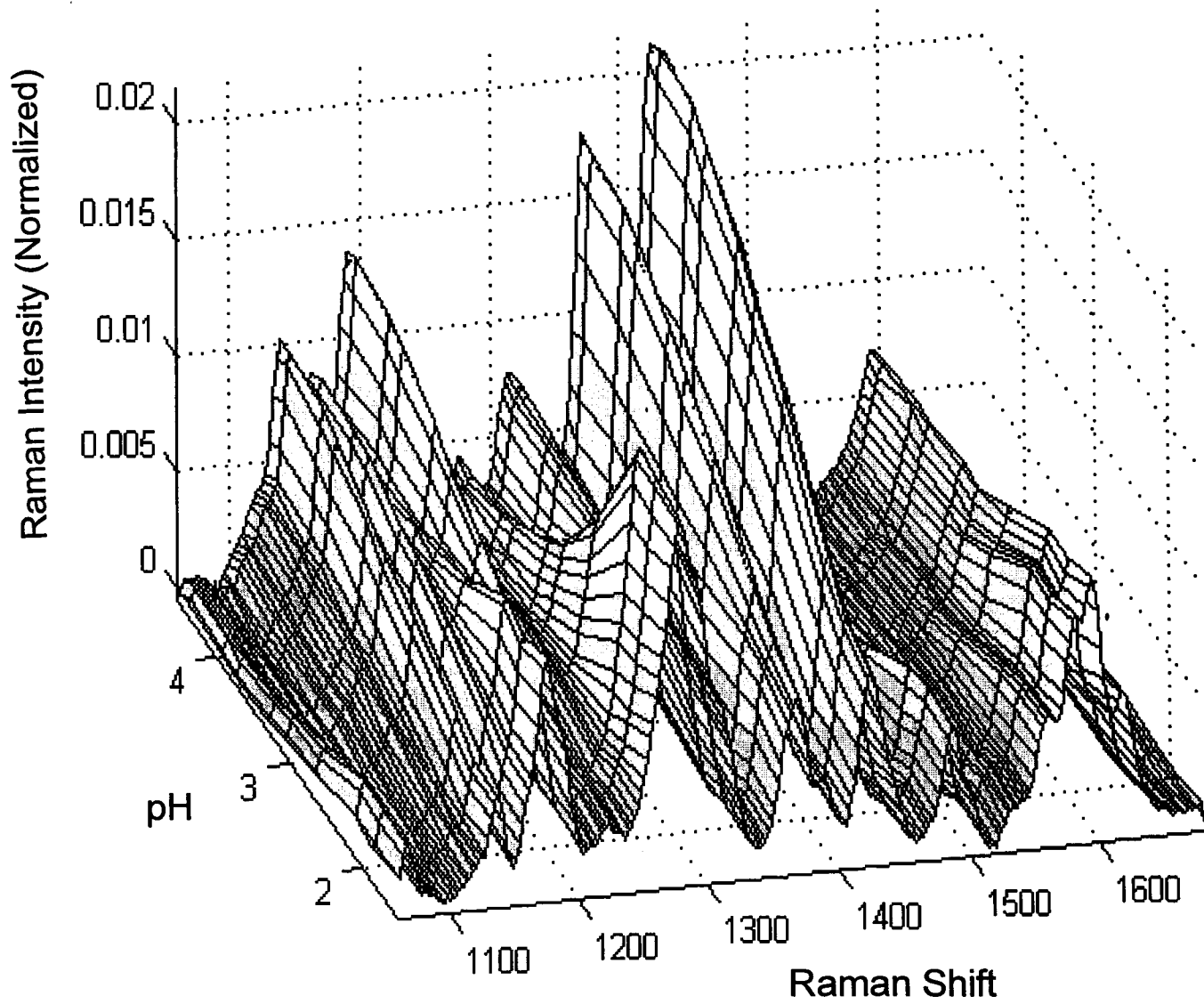












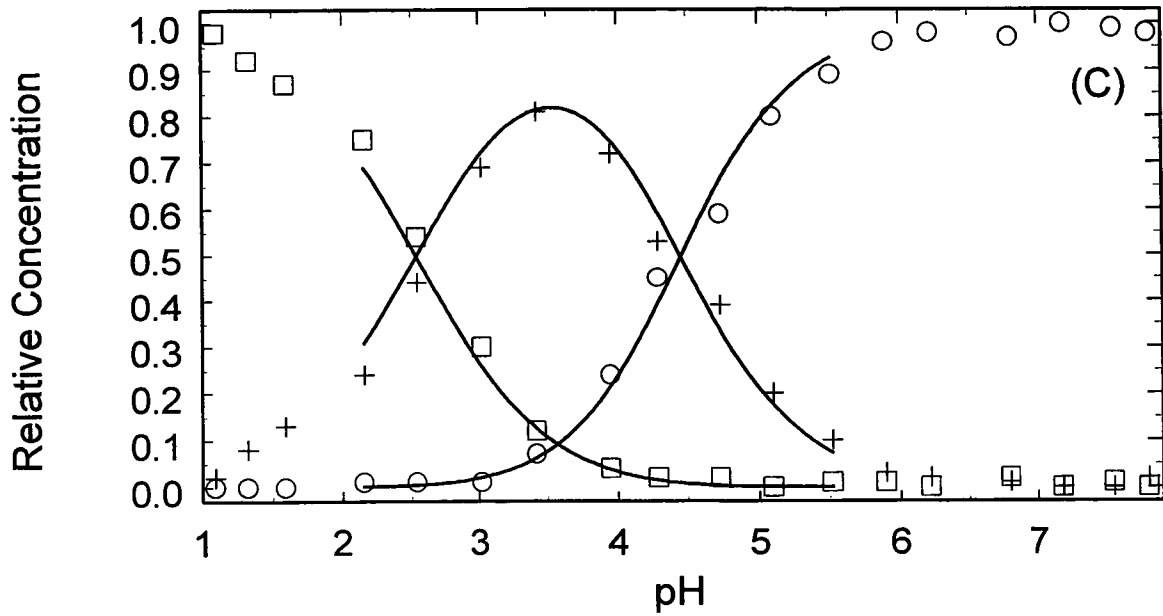
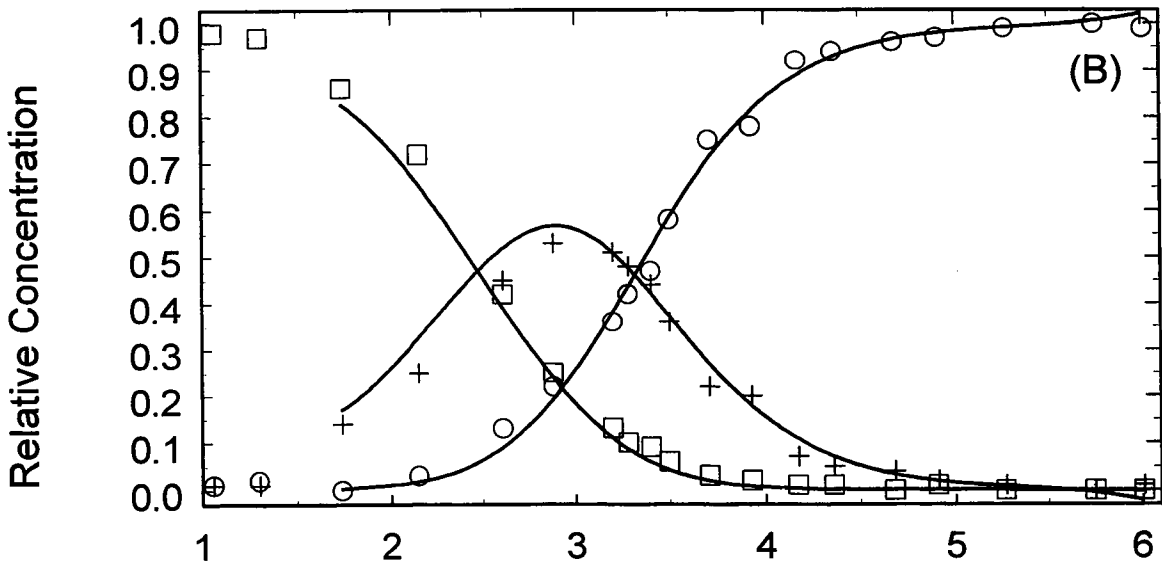
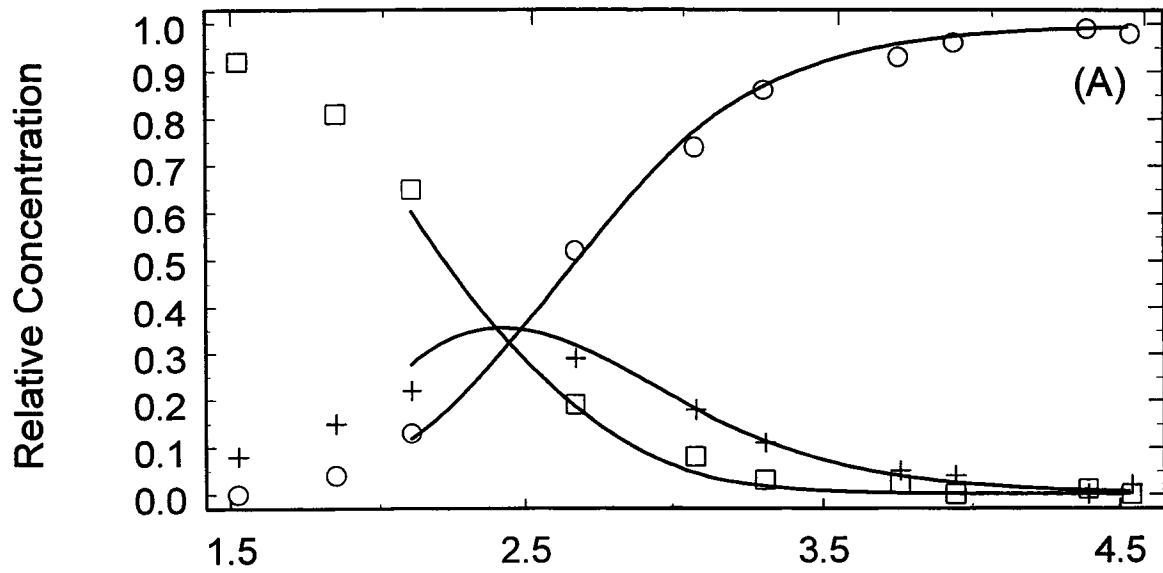


Figure 9

